PHYSICAL REVIEW B **79**, 161201(R) (2009)

Impact ionization in InSb probed by terahertz pump—terahertz probe spectroscopy

Matthias C. Hoffmann,[1,*] János Hebling,[2] Harold Y. Hwang,[1] Ka-Lo Yeh,[1] and Keith A. Nelson[1]
[1]*Massachusetts Institute of Technology, Cambridge, MA, 02139*
[2]*Department of Experimental Physics, University of Pécs, 7624 Pecs, Hungary*
(Received 28 December 2008; revised manuscript received 9 February 2009; published 6 April 2009)

Picosecond carrier dynamics in indium antimonide (InSb) following excitation by below band gap broadband far-infrared radiation was investigated at 200 and 80 K. Using a THz-pump/THz-probe scheme with pump THz fields of 100 kV/cm and an intensity of 100 MW/cm^2, we observed carrier heating and impact ionization dynamics. The number of carriers produced exceeds 10^{16} cm^{-3}, corresponding to a change in carrier density $\Delta N/N$ of 700% at 80 K. The onset of a well-defined absorption peak at 1.2 THz is an indication of changes in longitudinal optical (LO) and longitudinal acoustic (LA) phonon populations due to cooling of the hot electrons.

DOI: 10.1103/PhysRevB.79.161201 PACS number(s): 78.47.J−, 71.55.Eq, 72.20.Ht, 72.20.Jv

Indium antimonide (InSb) is a model system for the study of hot-electron dynamics due to its low band gap of 170 meV at room temperature[1] and the fact that it has the highest electron mobility and saturation velocity among all known semiconductors. The wealth of nonequilibrium transport phenomena that have been observed in this material[2–4] is of special interest due to the large nonparabolicity of the conduction band,[5] which results in negative differential mobility at comparatively low dc voltages and strong interactions of hot carriers with the LO phonon mode. Although the high mobility of InSb enables fabrication of transistors with extremely high switching speeds,[6] further technological applications are complicated by the low threshold for impact ionization. The elucidation of carrier dynamics on the ultrashort timescale is hence of great fundamental as well as technological interest. Impact ionization by electric fields is a well-known effect in InSb.[2] In bulk InSb, impact ionization is usually observed at relatively low dc fields of several hundred V/cm and occurs when the electron has acquired enough energy from the driving field to exceed the ionization threshold,[7] usually on the order of the band gap. The balance between the acceleration of carriers in an applied external field on one hand and the dissipation of energy by collisions with phonons[8] on the other hand plays a crucial role. Recently, high-intensity THz sources have made it possible to investigate impact ionization by purely optical methods. Intensity-dependent THz transmission measurement with 40 ns long pulses[9,10] and very recently *Z*-scan measurement with single-cycle pulses[11,12] have been performed. In the latter case the THz-pulse duration was as short as the characteristic electron momentum relaxation time $\tau \approx 1-10$ ps.

In this Rapid Communication, we report experimental observations of carrier generation in InSb at 80 and 200 K due to impact ionization induced by below band gap infrared (IR) radiation on the picosecond time scale, where $\omega\tau \approx 1$. Near single-cycle pulses with field strengths up to 100 kV/cm and a duration of 1 ps were used. The rise time of the THz pulses was less than the electron momentum relaxation time of $\tau = 2.5$ ps in InSb at 77 K. This leads to highly accelerated carriers that can cause carrier multiplication through impact ionization.[13] THz radiation can also be used as a very sensitive *probe* to directly monitor free-carrier behavior in semiconductors.[14] The combination of sub-band-gap direct excitation of doped semiconductors and time-resolved spectroscopy provides an excellent tool for observing carrier dynamics.[13,15]

The experimental setup shown in Fig. 1 was used for collinear THz-pump/THz-probe measurements. We generated single-cycle THz pulses by optical rectification of a 800 nm 5.5 mJ pulse from a Ti:sapphire laser with 100 fs pulse duration at a repetition rate of 1 kHz. We tilted the pulse intensity front with a grating-lens combination to achieve noncollinear velocity matching in lithium niobate,[16,17] yielding THz pulses with energies up to 3 μJ.[18,19] The optical beam was split using a 10:90 beamsplitter into two parts that were recombined under a small angle at the same spot on the grating. The 10% part was passed through a chopper wheel (not shown in figure) and was used to generate the THz probe. The 90% part was variably delayed and used to generate the THz-pump pulse. The single-cycle THz pulses were focused to 1 mm diameter at the sample using a 90° off-axis parabolic mirror pair with 190 and 75 mm focal lengths. Another off-axis parabolic mirror pair with focal lengths of 100 and 190 mm was used to image the sample plane onto the ZnTe detector crystal for electro-optic sampling of the THz field using balanced detection and a lock-in amplifier.[20] In order to ensure the linearity of the detected signal and to eliminate THz-pulse reflections,[21] the ZnTe sampling crystal had an active layer of 0.1 mm and a total thickness of 1.1

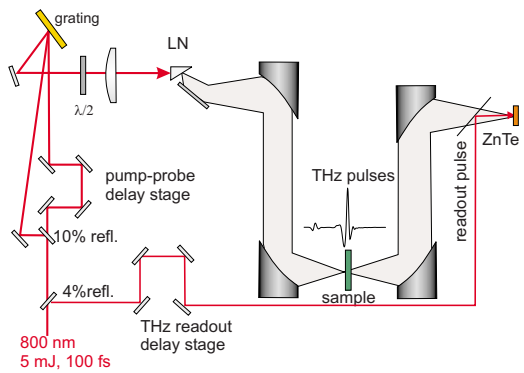

FIG. 1. (Color online) Schematic of the experimental setup. Collinear THz pulses are generated by tilted pulse front excitation in $LiNbO_3$ (LN) and detected electro-optically. See text for details.

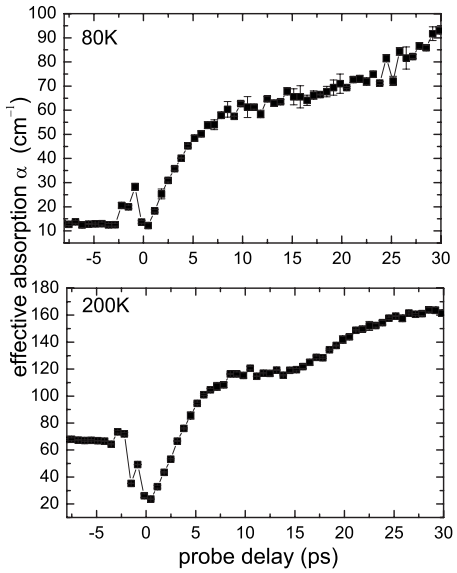

FIG. 2. THz-pump/THz-probe time-resolved absorption data, spectrally averaged over the 0.2–1.6 THz range, from doped InSb ($N=2.0\times10^{15}$ cm^{-3}) at 80 and 200 K. The deviation starting at 12 ps is due to reheating caused by the THz-pulse reflection within the sample.

mm. Selective chopping of the probe beam provided excellent suppression of the pump pulse. Spectral analysis of our THz-pump probe results was conducted in the 0.2–1.6 THz range where the spectral amplitude was sufficiently high. A pair of wire-grid polarizers was used to attenuate the THz pulses for intensity-dependent studies. The samples were a *n*-type Te doped and a nominally undoped InSb wafer, each 450 μm thick, with carrier concentrations at 77 K of 2.0×10^{15} and $2.0–4.9\times10^{14}$ cm^{-3}, respectively. The mobility at 77K as specified by the manufacturer was 2.5×10^{5} cm^2/Vs for the doped sample and 0.5×10^{6} cm^2/Vs for the undoped sample. The THz fields were polarized parallel to the (100) axes of the crystals. We measured the THz fields $E(t)$ that reached the ZnTe crystal with and without the sample in the beam path from which we calculated the effective absorption coefficient

$$\alpha_{\text{eff}} = -(1/d)\ln\{T^2[\textstyle\int_0^{t_{\max}} E_{\text{sam}}^2(t)dt/\int_0^{t_{\max}} E_{\text{ref}}^2(t)dt]\}, \quad (1)$$

where d is the sample thickness, $t_{\max}$ is the time window of the measurement, and T is a factor accounting for reflection losses at the sample surfaces. The quantity α_{eff} is equivalent to the energy absorption coefficient averaged over our bandwidth.

Figure 2 shows time-resolved absorption traces for the doped sample at 80 and 200 K covering a probe delay range of up to 30 ps. At both temperatures, the absorption increases after THz excitation and reaches a plateau after 30 ps with a total increase in absorption of 80–90 cm^{-1}. This rise is caused by the generation of new carriers through impact ionization. Unique to the measurement at 200 K is an initial dip in the absorption immediately after THz excitation. The drop in absorption in this case is caused by a decrease in the mobility of the hot electrons as a result of both the strong nonparabolicity of the Γ valley in the conduction band of InSb (Ref. 22) and scattering of these hot electrons into side valleys.[15,23,24] The carrier mobility μ directly influences the absorption coefficient α which is typically conceptualized by the Drude model and parametrized by the plasma frequency $\omega_p=(Ne^2/\epsilon_0\epsilon_\infty m^*)^{1/2}$ and the momentum scattering rate γ in the form $\alpha=\epsilon_\infty\omega_p^2\gamma/nc(\omega^2+\gamma^2)$, where ϵ_∞ is the high-frequency limit of the dielectric function and n is the refractive index. In the low-frequency limit ($\omega\ll\gamma$) the absorption α is directly proportional to the carrier mobility $\mu=e/\gamma m^*$. Due to the small band gap of InSb, the intrinsic carrier concentration at 200 K is much higher than that at 80 K. The effect of absorption saturation is thus much stronger at 200 K. After 4 ps, the additional absorption caused by the newly generated carriers exceeds the saturation effect, the magnitude of which is also diminishing as a result of the cooling of the hot carriers, thereby leading to the delayed rise observed in the overall absorption.

Comparison between the equilibrium absorption of InSb at 80 K and the value measured 30 ps after intense THz excitation shows an eightfold increase, indicating a similar increase in carrier concentration from 2×10^{15} to 1.6×10^{16} cm^{-3}. The same analysis cannot be applied reliably at 200 K due to the very large intrinsic carrier absorption, which overwhelms the dynamic range of our spectrometer system. This effect is especially acute at low frequencies where the absorption is strongest, leading to an apparent saturation of the frequency-averaged absorption shown in Fig. 2(b). Some signal at $t<0$ appears in Fig. 2(a) because of the nonlinear interaction in the LN crystal between the THz-pump and -probe fields and the optical pulses that generate them as well as nonlinear interactions in the sample.

We employed a simple system of rate equations, displayed below, to model the dynamics of impact ionization in the first 30 ps, assuming quadratic scaling[25] of the impact ionization probability above the threshold energy $\varepsilon_{\text{th}}\approx\varepsilon_g$,

$$(dN/dt) = C[\varepsilon(t)-\varepsilon_{\text{th}}]^2N(t)\Theta[\varepsilon(t)-\varepsilon_{\text{th}}], \quad (2)$$

$$(d\varepsilon/dt) = -C[\varepsilon(t)-\varepsilon_{\text{th}}]^2\varepsilon_{\text{th}}\Theta[\varepsilon(t)-\varepsilon_{\text{th}}]-(\varepsilon/\tau_\varepsilon). \quad (3)$$

In this model $N(t)$ is the electron concentration, $\varepsilon(t)$ is the average carrier energy, and $\Theta(t)$ is the Heaviside step function. We used a numerical value of $C=7\times10^{50}$ J^{-2} s^{-1} obtained by Devreese *et al.*[26] The energy relaxation time τ_e was assumed to be time and energy independent.

A numerical solution, taking into account the reflection at the sample interface, is shown in Fig. 3. The effect of absorption saturation due to carrier heating[15] was accounted for approximately by assuming $\alpha_{\text{eff}}\propto N(t)[\varepsilon_0-\varepsilon(t)]/\varepsilon_0$ where ε_0 is the average carrier energy immediately after excitation. From this fit we obtained a phenomenological relaxation time τ_ε time of 7 ps, much longer than the 1.3–2.0 ps calculated for the energy relaxation time in the dc limit by Kobayashi.[27]

Further intensity-dependent experimental results similar to the one shown in Fig. 3 indicate no observable absorption increase for single-cycle THz pulses with peak electric fields lower than 75 kV/cm. The threshold electric field in this case should be distinguished from that obtained in prior static or

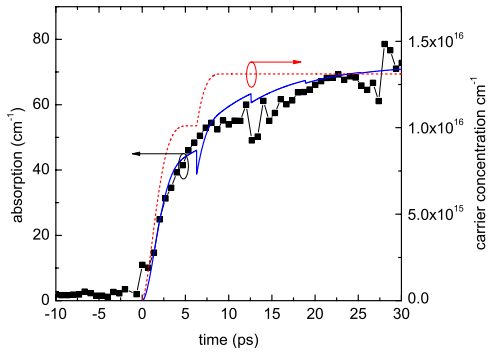

FIG. 3. (Color online) Experimental data for the undoped sample at 80 K (squares) and simulation results for the carrier concentration (dashed) and absorption (solid line) based on quadratic scaling of impact ionization rate with carrier energy. Parameters used were $N(t=0)=5\times10^{13}$ cm^{-3}, energy relaxation time $\tau_e=7$ ps, and $\varepsilon_0=\varepsilon(t=0)=1.3$ eV.

quasistatic measurements. An exponential increase in the carrier-generation rate was observed[28] in the 250–500 V/cm range and the rate saturated above 800 V/cm at a value as low as 0.007 ps^{-1}. In our opinion, ionization of shallow impurities, instead of band-to-band impact ionization, is responsible for this behavior. For a drift velocity of 4×10^7 cm/s in fields above 500 V/cm (Ref. 29) and the dependence of the avalanche multiplication on the electric field,[30] we are able to extrapolate a rate of 18 ps^{-1} for a static field strength of 48 kV/cm. The corresponding single-cycle generation rate of 18 ps^{-1} was obtained from the best fit of Fig. 3, in which a peak electric field of 100 kV/cm was used. Consequently, we observed that the peak field required for impact ionization by the single-cycle THz-pulse excitation is a factor of 2 larger than in the static field case. This difference can be attributed to the significantly shorter peak pulse duration compared to the momentum relaxation time in InSb and the fact that in Eqs. (2) and (3) we followed the average carrier energy and not an energy distribution.

In order to elucidate the lattice dynamics further, we performed a series of intensity-dependent pump-probe measurements with a fixed probe delay. Figure 4 shows the absorption spectra obtained with different pump intensities at a probe delay of 35 ps for the doped and undoped samples at 80K. At frequencies below 0.6 THz, we observe the expected Drude-type contribution from free-carrier absorption which is more pronounced at higher pump fluence. In addition, we observe a distinct absorption peak at 1.2 THz in the undoped sample and a weak feature that indicates a similar peak in the doped sample. The amplitude of the peak is highly intensity dependent and appears to approach its asymptotic value just above 50% of the maximum intensity. The behavior of this peak suggests that its origin is lattice vibrational rather than electronic. Polar-optical phonon scattering is well known as the dominant energy-loss mechanism for hot electrons in InSb.[31] The main channel of energy loss is through the emission of LO phonons with a frequency of 5.94 THz. These phonons decay into acoustic modes through anharmonic coupling and through the second-order electric moment of the lattice.[32] A series of sum and difference phonon peaks between 1 and 10 THz has been observed and assigned in the

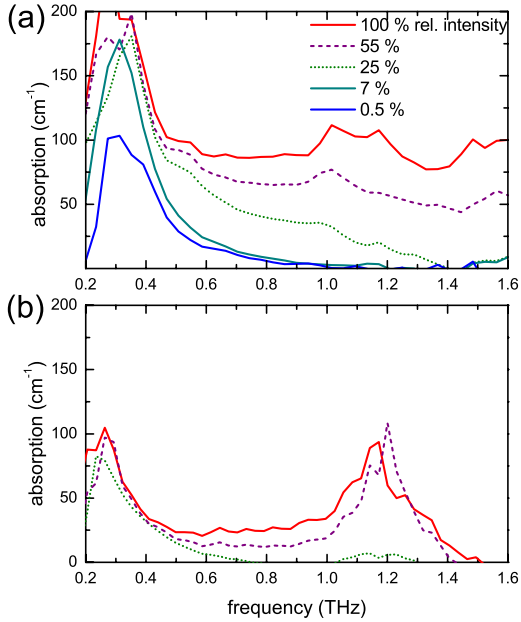

FIG. 4. (Color online) THz absorption spectra at various pump intensities measured at a probe delay time of 35 ps for the (a) doped sample and (b) undoped sample at 80 K.

far-infrared spectrum of InSb.[33] At very low THz fields, produced by a photoconductive antenna, we also were able to observe some of these weak absorption peaks in the undoped sample. The assignments reported[33] indicate a 1.2 THz difference frequency between the LO and LA modes at the zone boundary. The drastic change in the absorption coefficient of the difference phonon peak is the result of large changes in

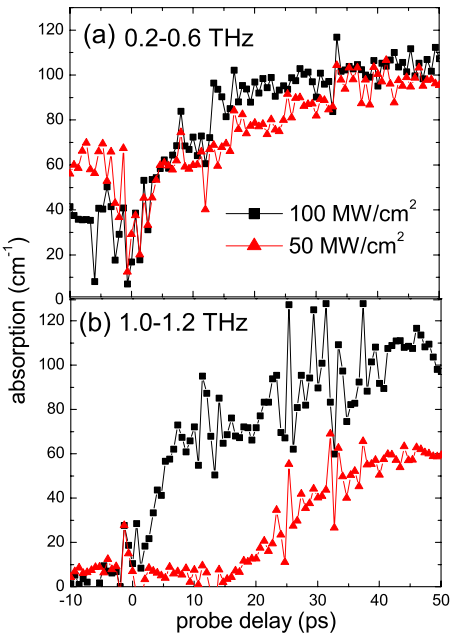

FIG. 5. (Color online) Time-resolved spectrally averaged absorption for the doped sample at 80 K with 100% pump intensity (squares) and 50% pump intensity (triangles). Spectrally averaged absorption is shown in the range (a) 0.2–0.6 THz and (b) 1.0–1.2 THz.

phonon populations due to energy transfer from the hot electrons generated by the THz-pump pulse. Monte Carlo simulations[34] have shown that substantial phonon population changes can occur even at comparatively low dc fields on picosecond timescales.

The temporal evolution of the electron-lattice interaction can be studied by separating the spectrally resolved pump-probe data into two different frequency bands: 0.2–0.6 and 1.0–1.2 THz. This is illustrated in Fig. 5 where data from time-resolved measurements at full THz intensity and at half the full intensity are shown for the doped sample. For the low-frequency band, the rise in absorption is almost identical at the two intensities, while the contribution from the absorption between 1.0 to 1.2 THz is reduced considerably when the THz intensity is halved. The higher-frequency portion of the absorption spectrum is clearly more sensitive to the intensity of the THz-pump pulse, as illustrated in Fig. 4(b). In addition, at the lower intensity there is a delay of approximately 10 ps before the rise of the absorption signal. This delay was reproduced qualitatively for all measurements at intermediate THz-pump levels. We do not have a complete understanding of the intensity dependence of the delay, but we note that the delay is on the order of the LO phonon decay time in InSb,[32] suggesting that it arises from LO phonon decay into LA phonons. The large fluctuations observed at 12 and 24 ps are due to THz-pump pulse reflections in the sample that are overlapped in the electro-optic crystal with the THz-probe pulse.

The presently developed THz-pump/THz-probe technique permits sensitive monitoring of carrier dynamics in semiconductors on the picosecond timescale. We observed the dynamics of impact ionization and carrier generation, up to a sevenfold increase over the equilibrium carrier generation, following intense THz excitation of InSb. Our ability to spectrally analyze the time-resolved signal allowed us to detect distinct features that we attribute decay of electronic energy into LO and LA modes. Monte Carlo simulations are needed for a more in-depth understanding of the interplay between hot electrons and lattice, taking into account effects such as impact ionization, intervalley- and polar-optical phonon scatterings, and changes in phonon population. Experimentally, a broader probe bandwidth exceeding 2 THz will enable us to monitor the phonon dynamics directly. Additional effects of the THz fields themselves, including the possibility of THz-induced band-to-band tunneling[35] that could produce new carriers directly, also warrant further analysis.

We would like to thank R. Brazis for stimulating discussions. This work was supported in part by ONR under Grant No. N00014-06-1-0463.

*mch@mit.edu

[1] D. G. Avery *et al.*, Proc. Phys. Soc. London, Sect. B **67**, 761 (1954).
[2] C. L. Dick and B. Ancker-Johnson, Phys. Rev. B **5**, 526 (1972).
[3] S. Asmontas *et al.*, Solid-State Electron. **31**, 701 (1988).
[4] R. D. Larrabee and W. A. Hicinbothem, IEEE Trans. Electron Devices **13**, 121 (1966).
[5] E. O. Kane, J. Phys. Chem. Solids **1**, 249 (1957).
[6] T. Ashley *et al.*, in Solid State and Integrated Circuits Technology , Proceedings of the 7th International Conference, Beijing, China, 2004.
[7] W. Shockley, Solid-State Electron. **2**, 35 (1961).
[8] S. D. Ganichev and W. Prettl, *Intense Terahertz Excitation of Semiconductors*, 1st ed. (Oxford University Press, New York, 2006).
[9] S. D. Ganichev *et al.*, Sov. Phys. JETP **63**, 256 (1986).
[10] S. D. Ganichev *et al.*, Appl. Phys. Lett. **64**, 1977 (1994).
[11] H. Wen *et al.*, in *Ultrafast Phenomena XVI*, edited by P. Corkum, S. de Silvestri, K. A. Nelson, E. Riedle, and R. W. Schoenlein (Springer, New York, 2008).
[12] H. Wen *et al.*, Phys. Rev. B **78**, 125203 (2008).
[13] M. C. Hoffmann *et al.*, in *Ultrafast Phenomena XVI*, edited by P. Corkum, S. de Silvestri, K. A. Nelson, E. Riedle, and R. W. Schoenlein (Springer, New York, 2008).
[14] M. C. Beard *et al.*, Phys. Rev. B **62**, 15764 (2000).
[15] J. Hebling *et al.*, in *Ultrafast Phenomena XVI*, edited by P. Corkum, S. de Silvestri, K. A. Nelson, E. Riedle, and R. W. Schoenlein (Springer, New York, 2008).
[16] J. Hebling *et al.*, Opt. Express **10**, 1161 (2002).
[17] T. Feurer *et al.*, Annu. Rev. Mater. Res. **37**, 317 (2007).
[18] K.-L. Yeh *et al.*, Opt. Commun. **281**, 3567 (2008).
[19] K.-L. Yeh *et al.*, Appl. Phys. Lett. **90**, 171121 (2007).
[20] Q. Wu and X.-C. Zhang, Appl. Phys. Lett. **67**, 3523 (1995).
[21] D. Turchinovich and J. I. Dijkhuis, Opt. Commun. **270**, 96 (2007).
[22] X. M. Weng and X. L. Lei, Phys. Status Solidi B **187**, 579 (1995).
[23] A. Mayer and F. Keilmann, Phys. Rev. B **33**, 6962 (1986).
[24] E. Constant, in *Hot Electron Transport in Semiconductors*, edited by L. Reggiani (Springer, New York, 1985).
[25] L. V. Keldysh, Sov. Phys. JETP **21**, 1135 (1965).
[26] J. T. Devreese *et al.*, Appl. Phys. A: Solids Surf. **29**, 125 (1982).
[27] T. Kobayashi, J. Appl. Phys. **48**, 3154 (1977).
[28] A. Krotkus and Z. Dobrovolskis, *Electrical Conductivity of Narrow-Gap Semiconductors* (Mokslas, Vilnus, 1988).
[29] R. Asauskas *et al.*, Sov. Phys. Semicond. **14**, 1377 (1980).
[30] V. V. Gavrushko *et al.*, Sov. Phys. Semicond. **12**, 1398 (1978).
[31] E. M. Conwell, *Solid State Physics, Suppl. 9* (Academic, New York, 1967).
[32] D. Ferry, Phys. Rev. B **9**, 4277 (1974).
[33] E. S. Koteles *et al.*, Phys. Rev. B **9**, 572 (1974).
[34] R. Brazis and R. Raguotis, Opt. Quantum Electron. **40**, 249 (2008).
[35] E. O. Kane, J. Phys. Chem. Solids **12**, 181 (1960).